

Multisampling Control of Two-Cell Interleaved Three-phase Grid-connected Converters

He, Shan; Zhou, Dao; Wang, Xiongfei; Blaabjerg, Frede

Published in:
2021 IEEE Applied Power Electronics Conference and Exposition (APEC)

DOI (link to publication from Publisher):
[10.1109/APEC42165.2021.9487390](https://doi.org/10.1109/APEC42165.2021.9487390)

Publication date:
2021

Document Version
Accepted author manuscript, peer reviewed version

[Link to publication from Aalborg University](#)

Citation for published version (APA):
He, S., Zhou, D., Wang, X., & Blaabjerg, F. (2021). Multisampling Control of Two-Cell Interleaved Three-phase Grid-connected Converters. In *2021 IEEE Applied Power Electronics Conference and Exposition (APEC)* (pp. 1432-1437). IEEE (Institute of Electrical and Electronics Engineers).
<https://doi.org/10.1109/APEC42165.2021.9487390>

General rights

Copyright and moral rights for the publications made accessible in the public portal are retained by the authors and/or other copyright owners and it is a condition of accessing publications that users recognise and abide by the legal requirements associated with these rights.

- Users may download and print one copy of any publication from the public portal for the purpose of private study or research.
- You may not further distribute the material or use it for any profit-making activity or commercial gain
- You may freely distribute the URL identifying the publication in the public portal -

Take down policy

If you believe that this document breaches copyright please contact us at vbn@aub.aau.dk providing details, and we will remove access to the work immediately and investigate your claim.

Multisampling Control of Two-Cell Interleaved Three-phase Grid-connected Converters

Shan He, Dao Zhou, Xiongfei Wang, and Frede Blaabjerg
 Department of Energy Technology, Aalborg University
 Aalborg 9220, Denmark
 she@et.aau.dk, zda@et.aau.dk, xwa@et.aau.dk, fbl@et.aau.dk

Abstract—This paper presents a multisampling control strategy for two-cell interleaved three-phase grid-connected converters in order to reduce the control delay and improve the stability margin. By sampling the currents at the point of common coupling, the average value can be acquired at the peak, valley and intersection points of all the phase-shifted carriers. Compared to the double-sampling double-update control, the bandwidth and dynamic performance improve with the same phase margin and no switching ripple is introduced at the same time. Finally, the effectiveness of the proposed control strategy is verified through the simulation and experimental results.

Keywords—Three-phase interleaved converter, bandwidth, multisampling control, dynamic performance.

I. INTRODUCTION

With the increase of power level of wind turbines, interleaved three-phase grid-connected converter is a potential solution due to its high efficiency and reliability compared to the single cell equivalent [1-2]. Specifically, the system capacity can be improved modularly with low current switching devices [3]. Furthermore, the total output current ripple is reduced with phase-shifted carriers. Consequently, the *LCL* filter can be replaced by *L* filter in order to improve the stability and decrease the cost [4].

For the control of interleaved three-phase grid-connected converter, there are mainly two kinds of methods. The first one is to control the output currents and circulating currents for each converter separately, which may cause instability due to the coupling between two control loops [5]. The other one is to control currents at the point of common coupling (PCC) to achieve power sharing, and the circulating current is suppressed by sampling the converter-side currents, respectively. As a result, there is no coupling between two control loops and the system stability can be improved [6]. However, control variables are usually sampled once or twice within one switching period for the above methods. Because the switching frequency is low in high power converters, the control bandwidth and dynamic performance are limited with the given stability margin [7]. Alternatively, multisampling control can reduce the control delay effectively, and it has been used in various converters to break the bandwidth limit [8]. It is worth noting that the switching ripple is also added in the control loop, and a digital filter is necessary to linearize the system [9]. The introduced phase lag will waste the advantage of phase boost, and the sampling frequency has to be higher to meet the stability margin requirement.

In this paper, a multisampling control strategy without sampling noise is proposed for the interleaved three-phase converter with an *L* filter. By multisampling the currents at

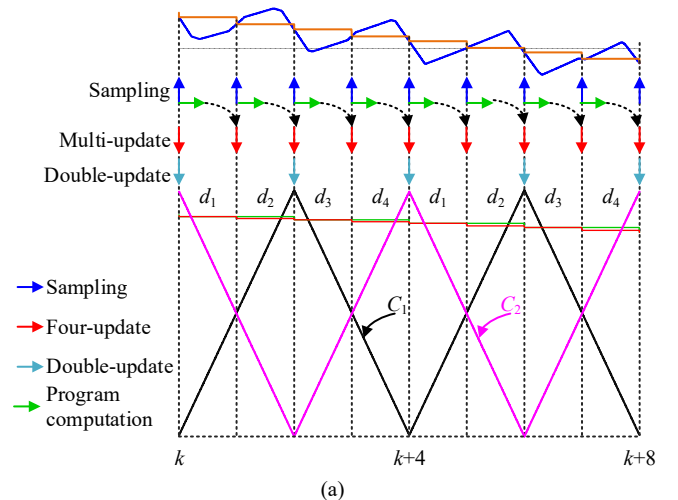
the point of common coupling (PCC), the average value can be acquired and the sampling frequency considering the number of cells is also discussed. Based on a two-cell interleaved converter, the bandwidth and dynamic performance comparison between the double sampling control and four-sampling control is presented. The circulating currents suppression under two different sampling modes is also discussed. Finally, the simulation and experimental results are presented to verify the effectiveness of the proposed strategy.

II. SAMPLING FREQUENCY SELECTION

If controlling every single cell of an interleaved converter separately, the average current can only be acquired at the peak and valley of the carrier. Moreover, the switching ripple will be introduced when using higher sampling frequency. Actually, the interleaved converter can be regarded as a multilevel converter, and the equivalent switching frequency is the product of the preset switching frequency and the number of interleaved cells. As a result, there is a sampling opportunity when controlling the currents at PCC directly. The average currents at PCC can be acquired at the peak, valley and intersection points of all the phase-shifted carriers, and the maximum sampling frequency without noise is

$$f_s = 2Nf_{sw} \quad (1)$$

where f_s , N , and f_{sw} is the maximum sampling frequency, number of interleaved cells and switching frequency, respectively. As shown in Fig. 1, for a two-cell interleaved converter, four-sampling control can be used and no switching ripple is introduced in the control loop.



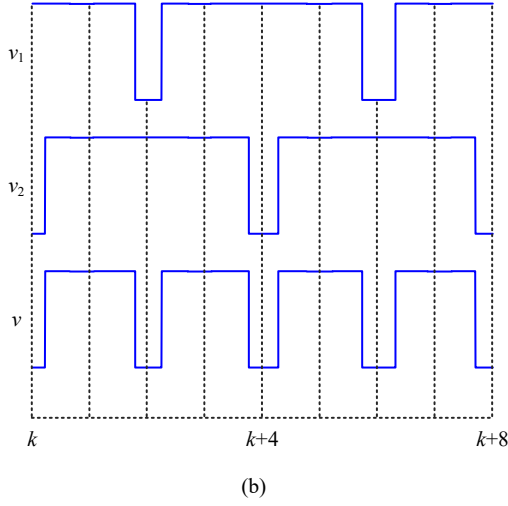


Fig. 1. Multisampling control principle of two-cell interleaved three-phase inverters. (a) Sampling process and modulation, (b) Pulse pattern.

If updating four times within one switching period, the average output voltage in the positive half fundamental period based on the voltage-second balance principle is

$$\begin{cases} i_{inv1}(k+4) - i_{inv1}(k) = L_{c1}(d_2 + d_3) \frac{u_{dc}}{2} \\ i_{inv2}(k+4) - i_{inv2}(k) = L_{c2}(d_1 + d_4) \frac{u_{dc}}{2} \end{cases} \quad (2)$$

where $i_{inv1} \sim i_{inv2}$, $L_{c1} \sim L_{c2}$, $d_1 \sim d_4$, u_{dc} are single-phase converter-side current for the first- and second-cell, converter-side inductance for the first- and second-cell, four updated duty ratios within a switching period, dc-link voltage, respectively. As a result, a low frequency circulating current appears in the converter-side currents for every single cell when circulating current controller is not used [10]. If ignoring the non-ideal factors such as filter-inductor variation and dead time difference, the average output voltage for every single cell can be same when adding circulating current suppressing loop. Actually, the same result can also be acquired if only updating twice within a switching period, and the average output voltage is given in (3). Hence, the four-sampling double-update control mode is selected in this paper.

$$\begin{cases} i_{inv1}(k+4) - i_{inv1}(k) = L_{c1}(d_1 + d_3) \frac{u_{dc}}{2} \\ i_{inv2}(k+4) - i_{inv2}(k) = L_{c2}(d_1 + d_3) \frac{u_{dc}}{2} \end{cases} \quad (3)$$

III. SINGLE-LOOP MUTISAMPLING CONTROL WITH PCC CURRENT FEEDBACK

In terms of current control, there is always a trade-off between the bandwidth and overshoot for the proportional integral (PI) controller, which weakens the advantage of multisampling. The pseudo-derivative-feedback controller is applied to substitute the PI controller in order to suppress the overshoot [11]. The single-loop control with PCC current feedback is used as a case study, and the overall control diagram is shown in Fig. 2.

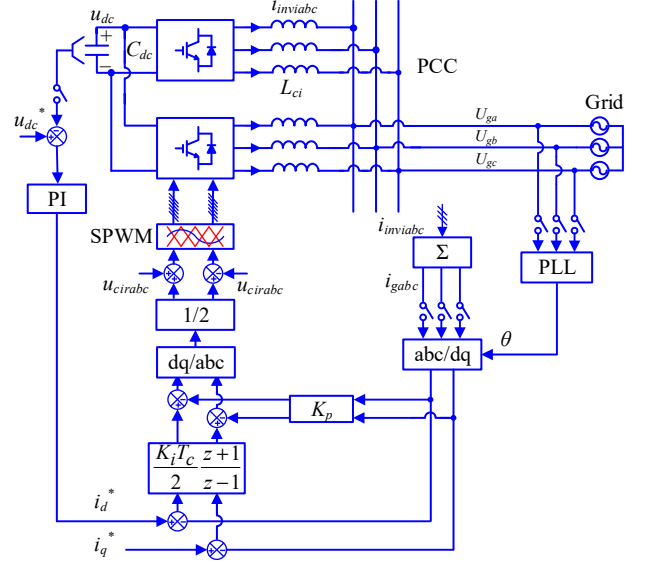


Fig. 2. Proposed control diagram. (a) Main current control loop, (b) Circulating current control loop.

Because the converter-side current sensors are necessary for system protection and circulating current suppression, the controlled PCC current can be calculated from the sampled converter-side currents in order to save cost. According to Fig. 3, the main current control loop stability is determined by the inner loop of current control loop, and its open-loop transfer function is

$$T_{oin} = \frac{K_p}{2} G_d(s) G_{igv}(s) \quad (4)$$

$$G_{igv}(s) = \frac{L_{c1} + L_{c2}}{sL_{c1}L_{c2}} \quad (5)$$

where $G_d(s) = e^{-0.5sT_{sw}}$. The equivalent filter inductance is halved if not considering filter inductor variation.

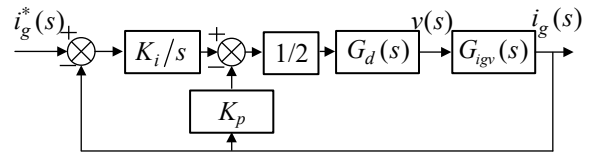


Fig. 3. Model of main current control loop diagram.

It is worth noting that the stability of the inner loop is same as the PI based single-loop control, and the bandwidth of the main current control loop is determined by the inner loop bandwidth and integral coefficient K_i . According to optimized controller design [12], when the same phase margin (PM) for the double-sampling control and four-sampling control is set to 45°, the bandwidth can be 333 Hz and 500 Hz, respectively, as shown in Fig. 4.

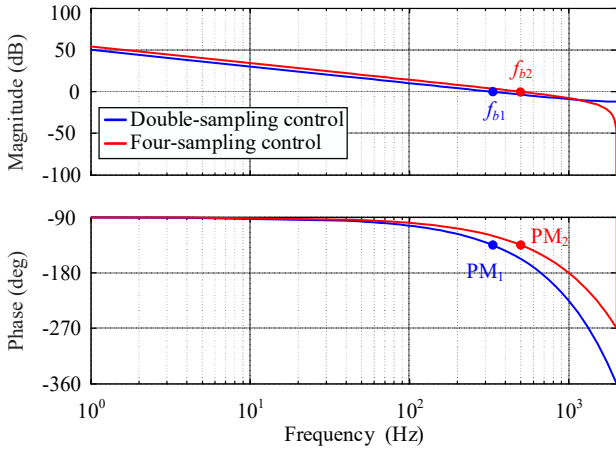


Fig. 4. Bode diagram of the inner loop of main current control loop.

Moreover, the reduced delay can be used to enhance the stability in weak grid. On the other hand, the bandwidth of the voltage control loop is set as 15 Hz. The overall parameters are shown in Table I.

TABLE I. MAIN PARAMETERS OF GRID-CONNECTED INVERTER

Symbol	Description	Value	Symbol	Description	Value
U_{dc}	DC-link voltage	200 V	U_g	Grid voltage	90 V
P_o	Output power	3 kW	L_c	Converter-side inductor	2 mH
f_s	Sampling frequency	4/8 kHz	f_{sw}	Switching frequency	2 kHz
C_{dc}	DC-link capacitor	594 μ F	T_{dead}	Dead time	3 μ s
K_{p2}	Proportional coefficient	4.1	K_{i2}	Integral coefficient	2000
K_{p4}	Proportional coefficient	6.6	K_{i4}	Integral coefficient	5000
K_{pc2}	Proportional coefficient	4.1	K_{ic2}	Integral coefficient	500
K_{pc4}	Proportional coefficient	4.1	K_{ic4}	Integral coefficient	500
K_{pdc}	Proportional coefficient	0.09	K_{idc}	Integral coefficient	3.25

On the other hand, the switching ripple will be introduced in the circulating current control loop when multisampling the converter-side currents, and a repetitive filter (RF) [9] can be used to remove them, as shown in Fig. 5.

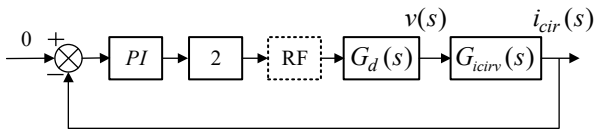


Fig. 5. Model of the circulating current control loop diagram.

The four-sampling open-loop transfer function for the circulating current control loop is

$$T_{ocir} = 2K_{pc} RF(s)G_d(s)G_{icirv}(s) \quad (6)$$

$$G_{icirv}(s) = \frac{1}{s(L_{c1} + L_{c2})} \quad (7)$$

where $G_d(s) = e^{-0.5sT_{sw}}$, $RF(s) = 0.5(1 + e^{-0.5sT_{sw}})$. The RF introduces 0.25 switching period delay, and the total control delay for the double-sampling and four-sampling circulating current control loop are equal to 0.75 switching period. As shown in Fig. 6, the bandwidth (333 Hz) and phase margin (45°) for both sampling modes are almost same. Hence, it is better to use double-sampling to suppress the circulating current, and the switching ripple can be fully removed.

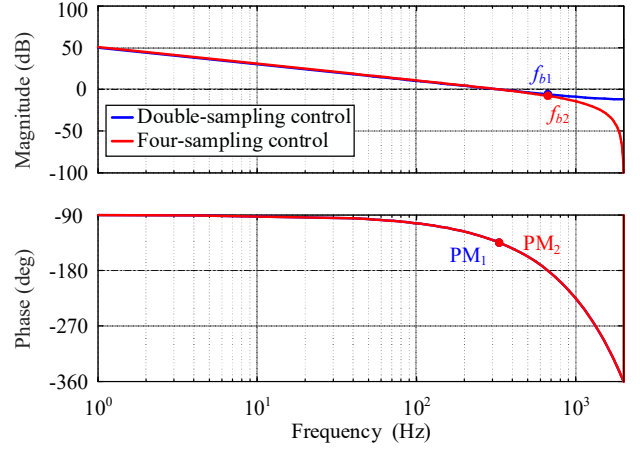
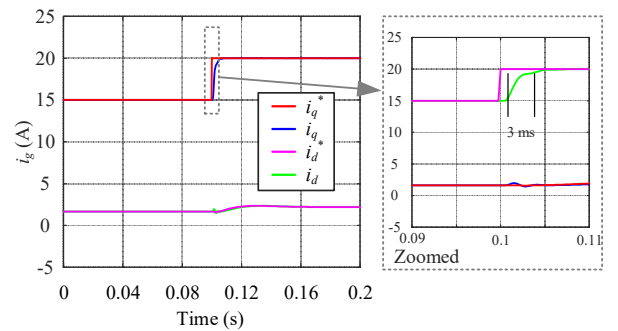


Fig. 6. Bode diagram of circulating current control loop.

IV. SIMULATION RESULTS

In order to illustrate the advantage of the multisampling control in terms of dynamic performance, the reference current steps from 15 A to 20 A (rated current) and the sampling frequency is set as 8 kHz. As shown in Fig. 7(a) and Fig. 8(a), the rising time (from 10% to 90% of the steady value) of the four-sampling four-update control improves from 3 ms to 1.75 ms compared with the double sampling control. Moreover, no switching ripple is introduced in the control loop when using four-sampling control. However, the low frequency circulating currents between two converters are large due to the different average output voltage, as shown in Fig. 8(b) and Fig. 8(c).



(a)

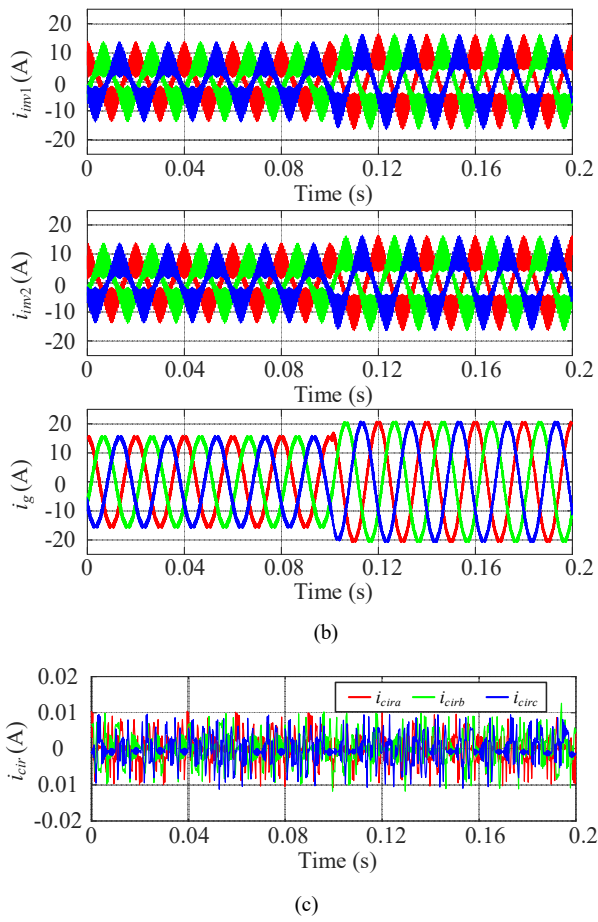


Fig. 7. Double-sampling double-update control with circulating current suppression. (a) Step response, (b) Analogue converter-side and PCC currents, (c) Low frequency circulating currents.

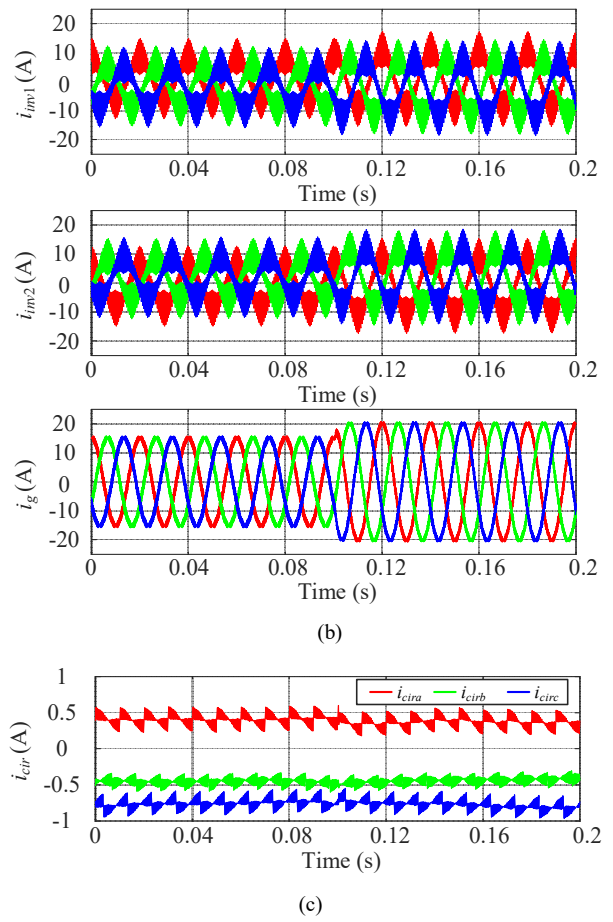
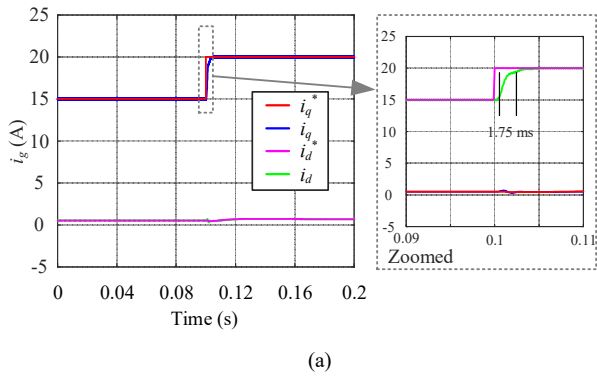
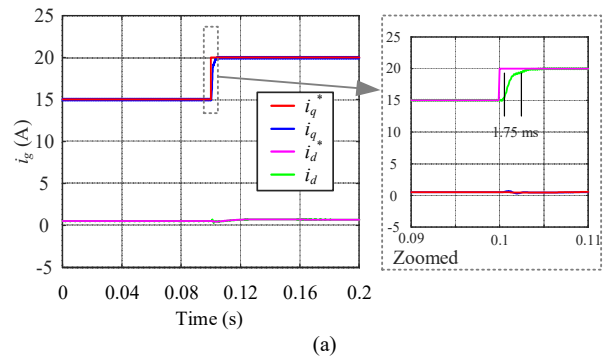


Fig. 8. Four-sampling four-update control without circulating current suppression. (a) Step response, (b) Analogue converter-side and PCC currents, (c) Low frequency circulating currents.



(a)



(a)

According to the above analysis, the average output voltage for the parallel two converters can be balanced when loading the duty ratio twice within one switching period. Moreover, double-sampling control is used in the circulating current control loop in terms of stability and switching ripple suppression. As shown in Fig. 9, a faster step response and a same low-frequency circulating current suppression performance are achieved compared with double-sampling double-update control.

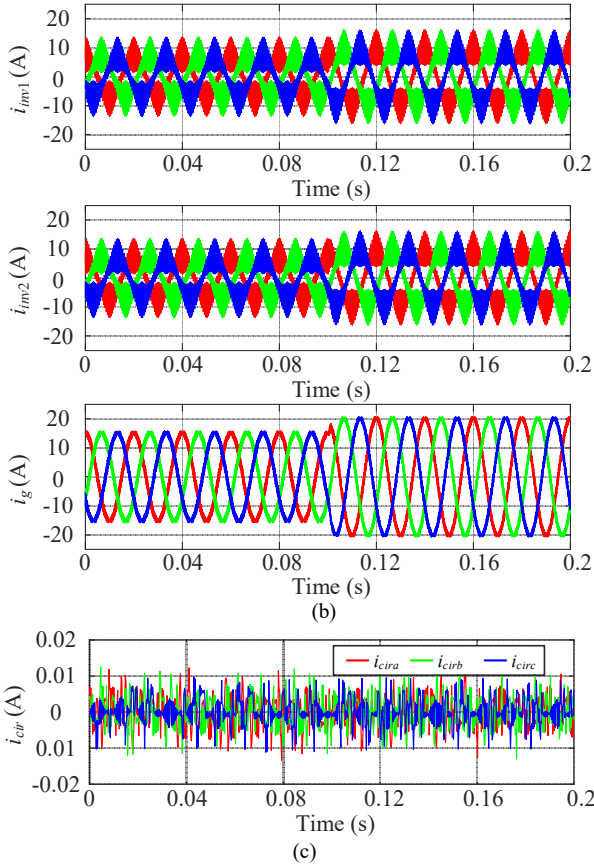


Fig. 9. Four-sampling double-update control with circulating current suppression. (a) Step response, (b) Analogue converter-side and PCC currents, (c) Low frequency circulating currents.

V. EXPERIMENTAL RESULTS

To further verify the theoretical analysis, experiments are carried out in a two-cell three-phase interleaved converter with an L filter, as shown in Fig. 10. The grid is emulated with a Chroma Grid Simulator Model 61845. The applied half-bridge module and the control platform are a PEB-8024 module and a B-BOX RCP control platform from Imperix, respectively.

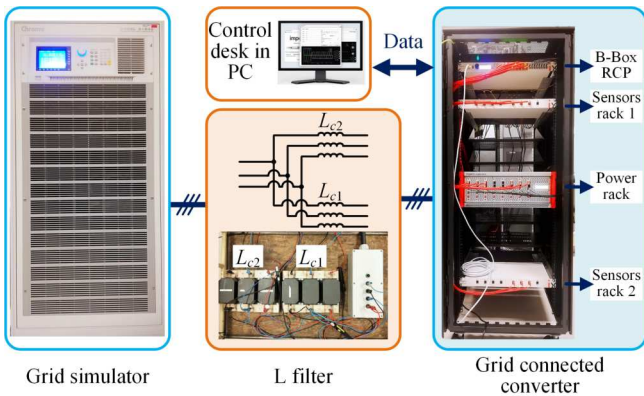


Fig. 10. Experimental setup.

The parameter for the setup can be seen in Table I. As shown in Fig. 11(a) and Fig. 12 (a), the noises in the d - and q -axis for the double-sampling control and four-sampling control are similar, and a better dynamic performance is achieved by the four-sampling control. Specifically, the

rising time of four-sampling control and double-sampling control is 3.28 ms and 1.91 ms, respectively. But the low-frequency circulating current is large when using four-sampling four-update control mode (without circulating current control), as shown in Fig. 11(c) and Fig. 12(c).

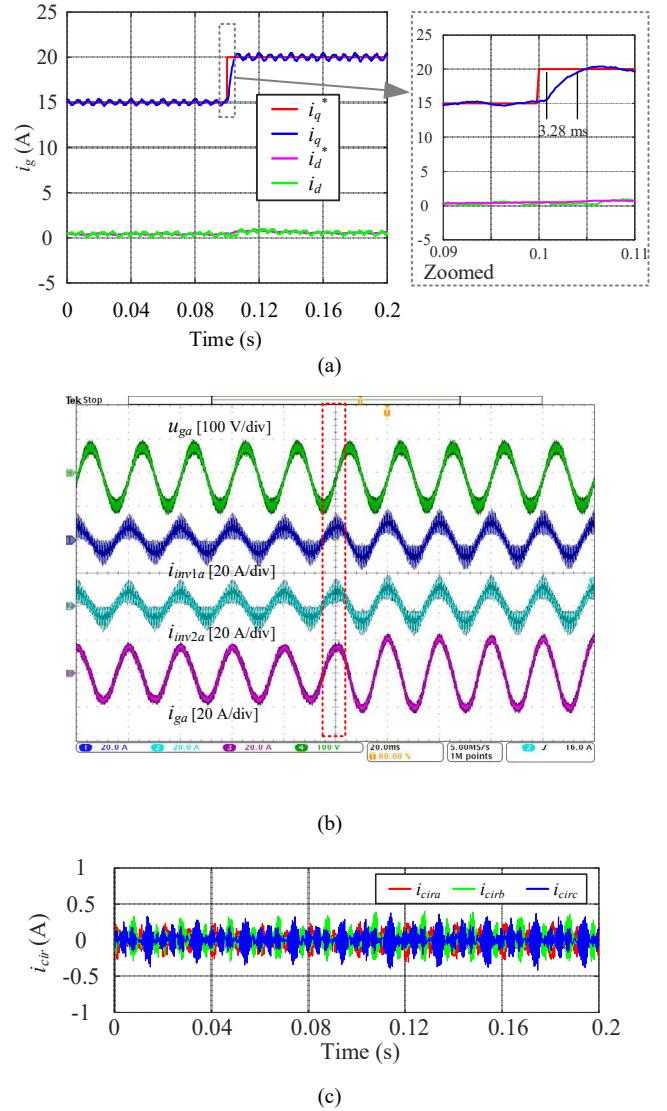
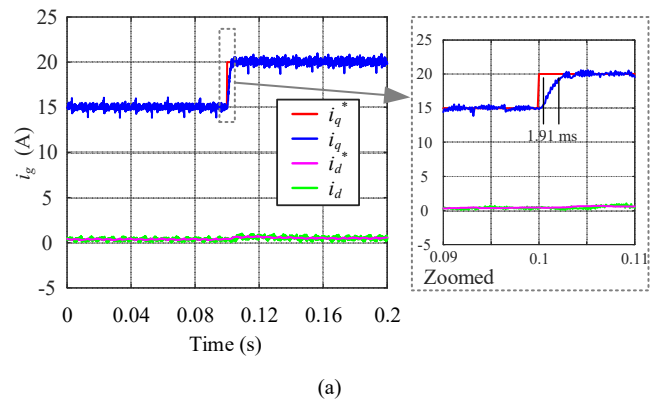
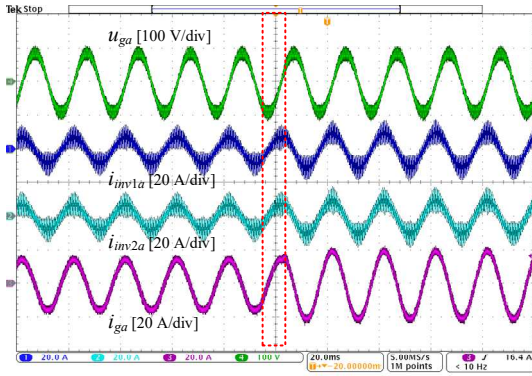


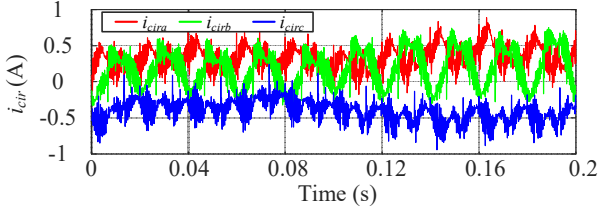
Fig. 11. Experimental results under double-sampling double-update control with circulating current suppression. (a) Step response, (b) converter-side currents and PCC currents, (c) Low frequency circulating currents.



(a)



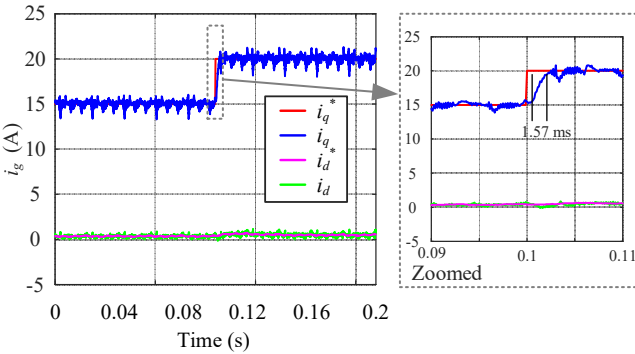
(b)



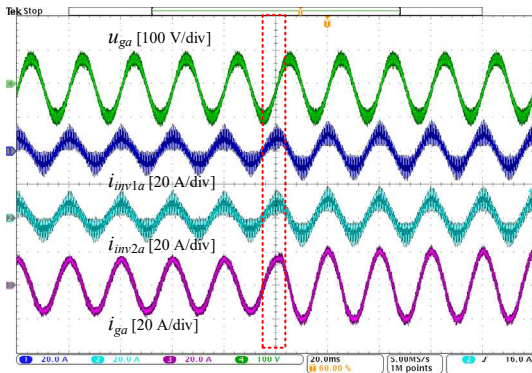
(c)

Fig. 12. Experimental results under four-sampling four-update control without circulating current suppression. (a) Step response, (b) Converter-side currents and PCC currents, (c) Low frequency circulating currents.

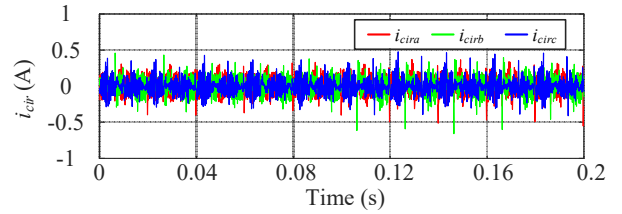
According to Fig. 13, when using four-sampling double-update control, the low-frequency circulating current can be suppressed because the average output voltage for two converters are same. Moreover, a faster current control response is achieved compared with double-sampling double-update control.



(a)



(b)



(c)

Fig. 13. Experimental results under four-sampling double-update control with circulating current suppression. (a) Step response, (b) Converter-side currents and PCC currents, (c) Low frequency circulating currents.

VI. CONCLUSIONS

In this paper, a multisampling control strategy for two-cell interleaved three-phase converters is proposed. The average current at PCC can be sampled at the peak, valley and intersection point of all the phase-shifted carriers. The duty ratio loading modes based on low-frequency circulating current suppression are discussed. Consequently, the bandwidth and dynamic performance are improved compared with the double-sampling double-update control. In the future, the proposed control strategy under weak grid will be investigated.

REFERENCES

- [1] R. Li and D. Xu, "Parallel operation of full power converters in permanent-magnet direct-drive wind power generation system," *IEEE Trans. Ind. Electron.*, vol. 60, no. 4, pp. 1619-1629, April 2013.
- [2] X. Zhang, W. Zhang, J. Chen, D. Xu, "Deadbeat control strategy of circulating currents in parallel connection system of three-phase PWM converter," *IEEE Trans. Energy Convers.*, vol. 29, no. 2, pp. 406-417, June 2014.
- [3] M. A. Abusara and S. M. Sharkh, "Design and control of a grid-connected interleaved inverter," *IEEE Trans. Power Electron.*, vol. 28, no. 2, pp. 748-764, Feb. 2013.
- [4] Z. Quan, Y. W. Li, Y. Pan, C. Jiang, Y. Yang and F. Blaabjerg, "Reconsideration of grid-friendly low-order filter enabled by parallel converters," *IEEE J. Emerg. Sel. Topics Power Electron.*, (early access), 2020.
- [5] Z. Ye, D. Boroyevich, J. Choi, and F. C. Lee, "Control of circulating current in two parallel three-phase boost rectifiers," *IEEE Trans. Power Electron.*, vol. 17, no. 5, pp. 609-615, Sep. 2002.
- [6] F. Wang, Y. Wang, Q. Gao, C. Wang and Y. Liu, "A Control Strategy for Suppressing Circulating Currents in Parallel-Connected PMSM Drives With Individual DC Links," *IEEE Trans. Power Electron.*, vol. 31, no. 2, pp. 1680-1691, Feb. 2016.
- [7] H. Tian, Y. W. Li and P. Wang, "Hybrid ac/dc system harmonics control through grid interfacing converters with low switching frequency," *IEEE Trans. Ind. Electron.*, vol. 65, no. 3, pp. 2256-2267, March 2018.
- [8] S. He, D. Zhou, X. Wang and F. Blaabjerg, "Overview of multisampling techniques in power electronics converters," in *45th Annual Conference of the IEEE Industrial Electronics Society (IECON)*, pp. 1922-1927, 2019.
- [9] L. Corradini, W. Stefanutti, and P. Mattavelli, "Analysis of multisampled current control for active filters," *IEEE Trans. Ind. Appl.*, vol. 44, no. 6, pp. 1785-1794, Nov.-Dec., 2008.
- [10] R. Maheshwari, G. Gohil, L. Bede and S. Munk-Nielsen, "Analysis and modelling of circulating current in two parallel-connected inverters," *IET Power Electron.*, vol. 8, no. 7, pp. 1273-1283, July 2015.
- [11] J. Wang, J. D. Yan, and L. Jiang, "Pseudo-derivative-feedback current control for three-phase grid-connected inverters with LCL filters," *IEEE Trans. Power Electron.*, vol. 31, no. 5, pp. 3898-3912, May 2016.
- [12] D. G. Holmes, T. A. Lipo, B. P. McGrath, and W. Y. Kong, "Optimized design of stationary frame three phase AC Current regulators," *IEEE Trans. Power Electron.*, vol. 24, no. 11, pp. 2417-2426, Nov. 2009.